Atti Soc. tosc. Sci. nat., Mem., Serie A, 115 (2010)
pagg. 9-15, figg. 3, tabb. 5; *doi: 10.2424/ASTSN.M.2010.02*

C. Biagioni (*), E. Bonaccorsi (*), S. Merlino (*)

CRYSTAL STRUCTURE OF BULTFONTEINITE, $Ca_4[SiO_3(OH)]_2F_2{\cdot}2H_2O$, FROM N'CHWANING II MINE (KALAHARI MANGANESE FIELD, REPUBLIC OF SOUTH AFRICA)

Abstract - The finding of well-crystallized specimens of bultfonteinite from the N'Chwaning II mine (Kalahari Manganese Field, Republic of South Africa) in the 1980s allowed the collection of new data about the crystal structure of this calcium silicate hydrate. The crystal structure study is in agreement with the general features outlined by McIver (1963) and allows the description of a reasonable hydrogen-bond scheme.

Key words - Bultfonteinite, C-S-H, crystal structure, N'Chwaning II mine, Republic of South Africa.

Riassunto - *Struttura cristallina della bultfonteinite, $Ca_4[SiO_3(OH)]_2F_2{\cdot}2H_2O$, dalla N'Chwaning II mine (Kalahari Manganese Field, Repubblica Sudafricana).* Il ritrovamento, negli anni Ottanta, di campioni ben cristallizzati di bultfonteinite nella miniera N'Chwaning II (*Kalahari Manganese Field*, Repubblica Sudafricana) ha permesso di raccogliere nuovi dati sulla struttura di questo silicato idrato di calcio. Lo studio strutturale ha consentito di confermare l'assetto generale descritto da McIver (1963) e di ipotizzare un ragionevole schema di legami a idrogeno.

Parole chiave - Bultfonteinite, C-S-H, struttura cristallina, N'Chwaning II mine, Repubblica Sudafricana.

Introduction

Bultfonteinite is quite a rare fluorine-bearing hydrated calcium nesosilicate. It was described by Parry *et al.* (1932) from the Bultfontein diamond mine (Republic of South Africa) where it was found at the beginning of the 20th century in a xenolith embedded in a kimberlite, associated with «apophyllite», calcite, and natrolite. Initially it was confused with this latter zeolite, but new findings in the Dutoispan and Jagersfontein diamond mines allowed Parry *et al.* (1932) to describe the new mineral species. As an alteration product of basaltic xenoliths embedded in kimberlitic rocks, bultfonteinite was also described from Lac de Gras (Canada; Chakhmouradian & Mitchell, 2001) and Damtshaa (Botswana; Buse *et al.*, 2010).

Murdoch (1955) described the occurrence of bultfonteinite at Crestmore (Riverside County, California, USA), in saccharoidal aggregates together with afwillite and scawtite. Successively, bultfonteinite was identified in the skarns of Mihara (Miyake, 1965) and Fuka (Kusachi *et al.*, 1997), both in Japan, and in the Hatrurim Formation (Israel; Gross, 1977), associated with tobermorite and afwillite. Bultfonteinite was also identified in the Wessels and N'Chwaning II mines (Kalahari Manganese Field, Republic of South Africa; Von Bezing *et al.*, 1991); its origin is related to an important hydrothermal process, known as the Wessels alteration event, occurred about 1.0-1.25 Ga ago (Gutzmer & Beukers, 1996).

The widespread twinning shown by bultfonteinite made the crystal structure determination difficult; the cell parameters were determined by Murdoch (1955), whereas Megaw & Kelsey (1955) identified the twin laws: according to them, twinning takes place according to axes normal to the (100) and/or (010) planes, with an angle between the two twin axes of about 90°. The determination of the crystal structure was performed by McIver (1963), using two-dimensional Fourier maps, achieving *R* indexes, for the [100], [010], and [001] projections, of 0.087, 0.095, and 0.114 respectively.

The well-crystallized specimens from the Kalahari Manganese Field, and in particular from the N'Chwaning II mine, allowed us to perform a new structural study, in order to fully characterize this phase. The aim of this paper is to illustrate the results of this crystal structure refinement and the description of the complex hydrogen bond scheme shown by bultfonteinite.

Experimental

Acicular colorless crystals of bultfonteinite were used throughout this study. These crystals are associated with a member of the series poldervaartite-olmiite. In the studied specimens, bultfonteinite can be associated also with oyelite; because of the morphological similarity between these two silicates, bultfonteinite was identified by X-ray powder diffraction using a 114.6 mm Gandolfi camera with Ni-filtered Cu$K\alpha$ radiation. Preliminary X-ray investigations by single-crystal oscillation and Weissenberg photographs showed that bultfonteinite is pseudo-orthorhombic, with cell parameters a 11.03, b 8.26, c 5.68 Å; the elongation direction is [001]. The hk0 layer showed reflections elongated parallel to the rotation axis, indicating that the studied crystal was formed by a parallel association on [001], with the single individuals slightly misaligned in the **ab** plane.

A small acicular crystal was selected and used for the intensity data collection performed at the CIADS (*Centro Interdipartimentale di Analisi e Determinazione Strut-*

(*) Dipartimento di Scienze della Terra, Università di Pisa, via Santa Maria 53, 56126 Pisa.

turale) of Siena University, using an Oxford Xcalibur S diffractomer with a CCD detector. The software CrysAlis[Pro] allowed the selection of reflections between two sets clearly belonging to twinned crystals. The refined cell parameters are *a* 10.999(1), *b* 8.176(1), *c* 5.6678(5) Å, α 94.24(1), β 89.00(1), γ 90.18(1)°, *V* 508.2(1) Å^3, space group $P\bar{1}$. A total of 2289 reflections was collected and corrected for Lorentz-polarization and absorption factors. The structure was refined using the SHELX software (Sheldrick, 2008) starting from the atomic coordinates given by McIver (1963), by accounting for a twinning through the TWIN instruction, adding a twin axis normal to (100). The isotropic refinement converged to R = 0.11; after the introduction of the anisotropy of thermal parameters, the R factor dropped to 0.087 for 1630 observed reflections. The refined ratio between the two individuals of the twinned crystals is 84:16. Table 1 reports the details of the data collection and the crystal structure refinement.

Structure description

General features

Table 2 shows atomic coordinates, equivalent displacement parameters and site occupancies, whereas Table 3 reports the bond distances. The atomic coordinates are in agreement with those reported by McIver (1963). The crystal structure of bultfonteinite presents four independent Ca sites and two independent Si sites. The Ca sites have a seven-fold coordination, with an average bond distance around 2.40 Å; Ca-O distances range from 2.304(6) Å (Ca3-O7 bond) to 2.560(7) Å (Ca3-O8 distance). These bond lengths are in agreement with those given by McIver (1963), ranging from 2.31(2) to 2.59(2) Å. The coordination polyhedra of Ca sites can be described as a monocapped trigonal prism; the capping ligands are O9, O10, O5, and O6 for the four independent Ca sites, respectively. The average Si-O distance is 1.632 and 1.631 Å for Si1 and Si2 sites, respectively; the bond lengths range from 1.596(6) to 1.654(7) Å.

The crystal structure of bultfonteinite can be described as formed by two kinds of layers, stacked along [010] (Fig. 1).

The first layer (layer A; Fig. 2a) is composed by Ca1, Ca2, Si1, and Si2 polyhedra. Ca1 and Ca2 share edges, forming ribbons running along [001], with the alternation of Ca1 and Ca2 sites. Every ribbon has the anionic sites O9 and O10 (the capping ligands of the Ca polyhedra) pointing in the same direction; adjacent ribbons have these sites pointing in the opposite direction. The layer assumes a wavy character. Every ribbon is connected to the adjacent ones by Si tetrahedra and hydrogen bonds. The second layer (layer B; Fig. 2b) is formed by Ca3 and

Tab. 1 - Crystal data and details of intensity data collection and structure refinement.

Dati cristallografici	
Chemical formula	$Ca_4[SiO_3(OH)]_2F_2 \cdot 2H_2O$
Crystal size (mm^3)	0.5 x 0.05 x 0.05 mm^3
Symmetry, space group	Triclinic, $P\bar{1}$
a, *b*, *c* (Å); α, β, γ (°)	10.999(1), 8.176(1), 5.6678(5); 94.24(1), 89.00(1), 90.18(1)
V (Å^3)	508.2(1)
Z	2
Raccolta e raffinamento strutturale	
Radiation, wavelenght (Å)	Mo$K\alpha$, λ = 0.71073
Temperature (K)	293
Sample-detector distance (mm)	45
Maximum observed 2θ	58.06
Measured reflections	3796
Unique reflections	2289
Observed reflections ($F_o > 4\sigma F_o$)	1630
R_{int}	0.0429
h, *k*, *l* range	$-14 \le h \le 14$, $-5 \le k \le 11$, $-7 \le l \le 6$
R [F_o>4 σ F_o]	0.0868
R (all reflections)	0.1056
wR_2 (on F_o^2)	0.2286
Goof	1.016
Number of refined parameters	164

Tab. 2 - Atomic coordinates and equivalent displacement parameters.

Site	*x*	*y*	*z*	U_{eq}	Site occupancy
Ca1	0.1326(2)	0.7934(2)	0.7841(3)	0.0108(4)	Ca
Ca2	0.3686(2)	0.7940(2)	0.2849(3)	0.0107(4)	Ca
Ca3	0.1195(2)	0.4778(2)	0.2492(3)	0.0105(4)	Ca
Ca4	0.3820(2)	0.4804(2)	0.7467(3)	0.0105(4)	Ca
Si1	0.4280(2)	0.2392(3)	0.2142(4)	0.0091(6)	Si
Si2	0.0701(2)	0.2393(3)	0.7278(4)	0.0089(6)	Si
F1	0.2513(5)	0.6226(6)	0.0130(9)	0.0122(11)	F
F2	0.2490(5)	0.6230(6)	0.5118(9)	0.0113(11)	F
O3	0.0438(6)	0.0413(8)	0.6971(10)	0.0132(13)	O
O4	0.4563(6)	0.0400(8)	0.1965(11)	0.0152(14)	O
O5	0.2810(6)	0.2685(8)	0.1897(10)	0.0133(14)	O
O6	0.2172(6)	0.2688(8)	0.7540(10)	0.0119(13)	O
O7	0.0101(6)	0.3214(7)	0.5005(11)	0.0120(13)	O
O8	0.0069(4)	0.3184(3)	0.9647(10)	0.0112(13)	O
O9	0.1908(6)	0.9587(8)	0.1603(11)	0.0196(15)	O
O10	0.3102(6)	0.9564(9)	0.6566(12)	0.0205(15)	O
O11	0.5066(6)	0.6809(7)	0.0034(10)	0.0094(12)	O
O12	0.4867(6)	0.3208(7)	0.4580(10)	0.0112(13)	O

Ca4 polyhedra. They form ribbons running along [001], with alternation of Ca3 and Ca4. As observed in the layer A, ribbons with the capping ligands (O5 and O6) pointing in a direction are linked by edge-sharing to ribbons having these sites pointing in the opposite direction. Therefore, an infinite two-dimensional wavy layer is formed. The connection between layer A and B is achieved through edge-sharing between Ca polyhedra belonging to the two layers and through the sharing of an edge of the Si tetrahedron.

The hydrogen bond scheme

Table 4 shows the bond-valence balance calculation, following Brese & O'Keeffe (1991). The total sum of

Tab. 3 - Selected bond distances (in Å).

Ca1	-O8	2.308(6)	Ca2	-O4	2.313(7)	Si1	-O11	1.596(6)
	-O3	2.342(6)		-O11	2.326(6)		-O12	1.632(6)
	-F2	2.363(5)		-F2	2.353(5)		-O5	1.645(7)
	-F1	2.383(6)		-F1	2.397(6)		-O4	1.654(7)
	-O7	2.409(7)		-O12	2.415(7)		average	1.632
	-O10	2.488(8)		-O10	2.481(7)			
	-O9	2.529(7)		-O9	2.518(7)			
	average	2.403		average	2.400			
Ca3	-O7	2.304(6)	Ca4	-O12	2.310(6)	Si2	-O8	1.596(6)
	-F1	2.335(5)		-F1	2.318(5)		-O3	1.641(7)
	-F2	2.336(5)		-F2	2.362(6)		-O6	1.642(7)
	-O8	2.362(6)		-O11	2.365(6)		-O7	1.644(7)
	-O5	2.472(6)		-O6	2.504(6)		average	1.631
	-O7	2.518(6)		-O12	2.507(6)			
	-O8	2.560(7)		-O11	2.527(6)			
	average	2.412		average	2.413			

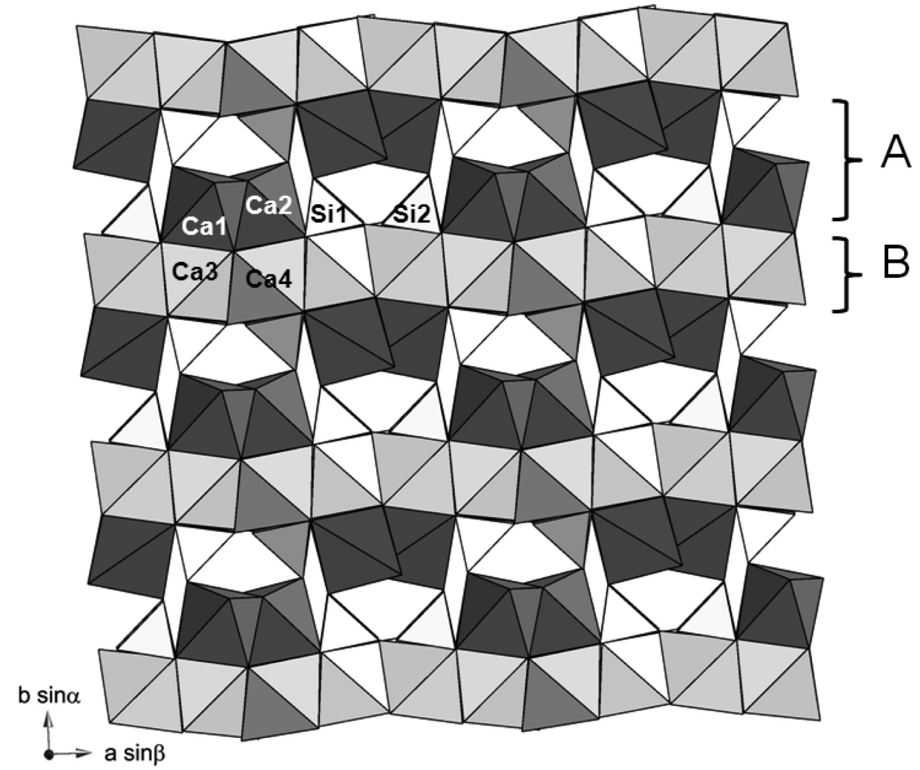

Fig. 1 - Crystal structure of bultfonteinite, as seen down [001].

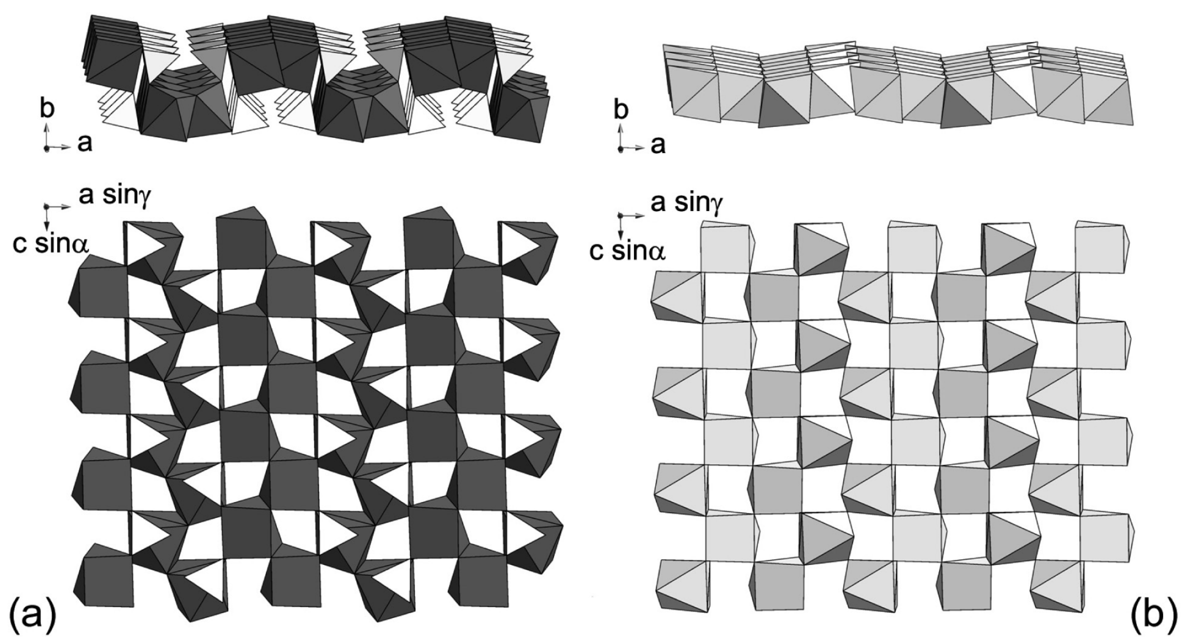

Fig. 2 - The two layers forming the crystal structure of bultfonteinite. The layers A (a) and B (b) are shown along the normal to (001) and down [010].

Tab. 4 - Bond valence balance calculations.

	Ca1	**Ca2**	**Ca3**	**Ca4**	**Si1**	**Si2**	**Σ anions**	**Σ' corr**	**Σ'' corr**	**species**
F1	0.23	0.22	0.26	0.28			0.99			F
F2	0.24	0.25	0.26	0.24			0.99			F
O3	0.36					0.95	1.31	1.54	1.92	O
									1.16	OH
O4		0.39			0.92		1.31	1.53	1.11	OH
									1.95	O
O5			0.26		0.94		1.20	1.42	1.72	O
									1.12	OH
O6				0.23		0.95	1.18	1.38	1.08	OH
									1.68	O
O7	0.30		0.63			0.95	1.88			O
O8	0.40		0.55			1.08	2.03			O
O9	0.22	0.23					0.45	0.00		H_2O
O10	0.24	0.25					0.49	0.07		H_2O
O11		0.38		0.56	1.08		2.02			O
O12		0.30		0.63	0.98		1.91			O
Σ cations	1.99	2.02	1.96	1.94	3.92	3.93				

Note: Σ (column 8) gives the sum of the valence-bond contributions from cations; Σ' (column 9) reports the valence sums corrected for the hydrogen bond contribution of the water molecules O9 and O10; Σ'' (column 10) reports the valence sums for O3, O4, O5, and O6.

valence-unit (*vu*) for the cations does not differ more than 3% from the ideal values. The monovalent character of F1 and F2 sites is confirmed, indicating the preferential occupancy of these sites by fluorine anions. The anionic sites O7, O8, O11, and O12 have a total sum of valence units between 1.88 and 2.03 *vu*, indicating that these sites are occupied by oxygen. The low values of O9 and O10 sites suggest an occupancy by H_2O molecules, whereas the actual nature of the O3 to O6 sites, with valence-unit sums between 1.18 and 1.31 *vu*, will be understood after a careful examination of the O···O distances, which may suggest a reliable scheme of hydrogen bonds.

Table 5 reports the O···O distances shorter than 2.8 Å between oxygen atoms not linked to the same cation; the table reports also the corresponding bond strengths of possible hydrogen bonds, expressed in *vu*, calculated according to Ferraris & Ivaldi (1988).

Both the two H_2O molecules O9 and O10 are involved in hydrogen bonds with O3 to O6 anions, linked to Si atoms. In all these cases, H_2O molecules behave as donor. O3 to O6 sites achieve a total sum ranging from 1.38 to 1.54 *vu*.

Taking into account the O···O distances involving these four anionic sites, a reasonable hydrogen bond scheme could be proposed. O3 and O6 belong to Si2 tetrahedron, whereas O4 and O5 belong to Si1 tetrahedron. It could be hypothesized that in the strong hydrogen bond O3···O3, one of the two sites is occupied by an oxygen atom, the other by a hydroxyl group: the O6 site, belonging to the same tetrahedron, should be a hydroxyl group whenever O3 is an oxygen atom, whereas it should be an oxygen anion if O3 site hosts a hydroxyl group. An analogous situation occurs for the O4 and O5 sites. There are two possible schemes of hydrogen bonds, indicated with 1 and 2, respectively, in Figure 3, ordered along [101]. Adjacent ribbons in the same layer A may present the same scheme or opposite hydrogen bond pattern. The disordered sequence of hydrogen bond scheme is not limited only to a single layer but different A layers may show different sequences of hydrogen bond schemes.

It is important to stress that the inversion centre is a consequence of the equi-probability of the occurrence of the O3-H···O3 and O3···H-O3 bonds; the obtained $P\bar{1}$ symmetry of the whole structure is the result of the disordered distributions of the two ordered hydrogen bond schemes. The tetrahedra correlated by the inversion point are no more equivalent in each ordered domain, showing a different distribution of hydroxyl groups. Obviously, the ordered distribution of O/OH could be inverted, obtaining an alternative hydrogen bond scheme.

Discussion

Taking into account the presence of a hydroxyl group for each tetrahedron, the chemical formula of bultfonteinite may be written as $Ca_4[SiO_3(OH)]_2F_2·2H_2O$, in agreement with the chemical data reported by the previous authors.

Tab. 5 - O···O distances and bond strength.

	d(Å)	v.u.		d(Å)	v.u.
O3-O3	2.494(12)	0.38	O3-O9	2.690(9)	0.23
O4-O4	2.456(12)	0.42	O5-O9	2.712(10)	0.22
O5-O6	2.579(9)	0.30	O4-O10	2.713(10)	0.22
			O6-O10	2.768(9)	0.20

Together with afwillite, poldervaartite, and olmiite, bultfonteinite is one of the rare nesosilicates characterized by $SiO_3(OH)$ groups. A scrutiny of the crystal structure of afwillite (Malik & Jeffery, 1976), poldervaartite (Dai *et al.*, 1993), and olmiite (Bonazzi *et al.*, 2007), reveals that Si-OH bond distances are longer than Si-O. Nyfeler & Armbruster (1998) observed that the average Si-OH bond distance in nesosilicates is 1.668 Å, whereas the average Si-O bond distance is 1.62 Å. In the two independent Si sites of afwillite, the Si-OH bond distance is respectively of 1.688 and 1.674 Å, while the average Si-O bond distance is 1.616 and 1.619 Å. In poldervaartite and in its isotype, olmiite, Si-OH distances are 1.697 and 1.675 Å respectively, while the average Si-O bond distances are 1.616 and 1.619 Å. It is interesting to note that in bultfonteinite this difference between Si-OH and Si-O bond distances cannot be appreciated. A possible explanation is related both to the 50% occurrence of hydroxyl groups in O3 to O6 sites and to the disordered distribution of O/OH in following layers; the averaging effect of X-ray diffraction studies does not allow to appreciate the difference, giving a mean position of O atoms.

The relatively high *R* value may be related not only to this structural disorder but also to the widespread twinning, not completely accounted for, as indicated by the presence of residual maxima in the difference Fourier map, having the same *x*, *y* coordinates of the refined atoms but ± 0.20 shifted *z* coordinates.

Even if the cell parameters could suggest a mono-

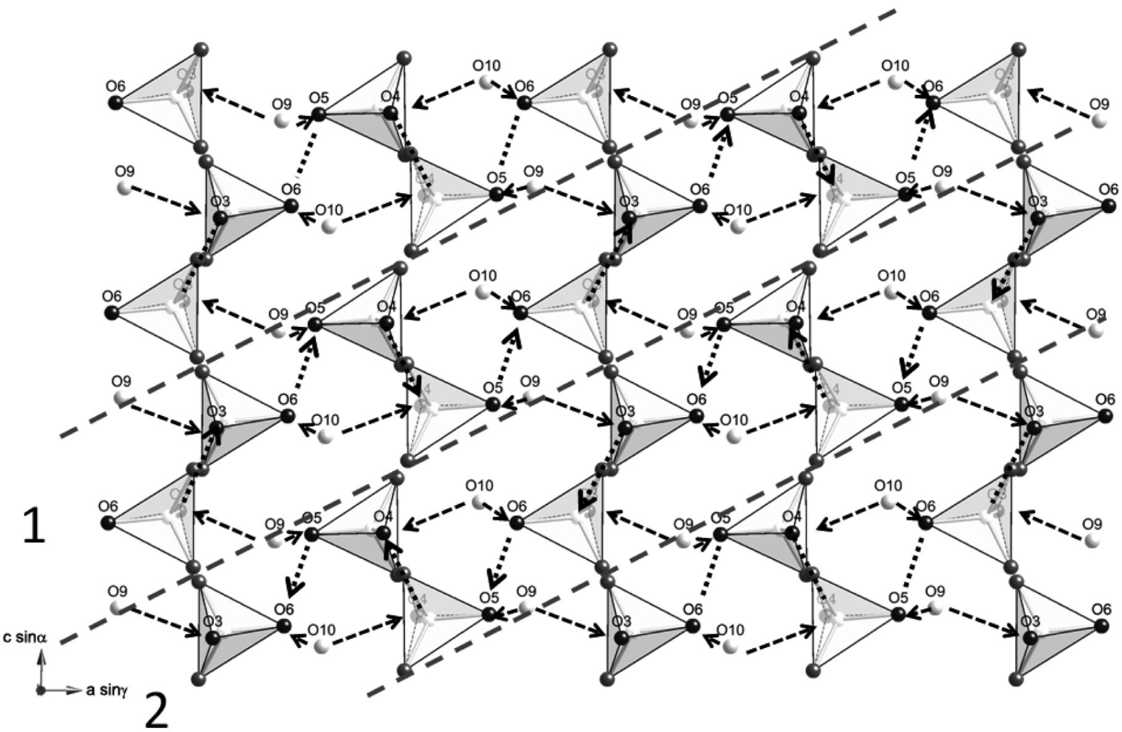

Fig. 3 - The complex hydrogen bond scheme in bultfonteinite, as seen along **b**. The hydrogen bonds are ordered in ribbons along [101]. Two different schemes are possible (1 and 2): in ribbon 1, O6 are OH^- anions, while O5 are O^{2-}; on the contrary, in ribbon 2, O5 are OH^- and O6 are O^{2-} anions. O3 and O4 are OH^- and O^{2-} in both these ribbons but in ribbon 1 the O3 pointing up are O^{2-} anions and those pointing down are OH^-; the O4 sites pointing up are a OH^-, while those pointing down are O^{2-}. The opposite situation occurs in ribbon 2. Adjacent ribbons may present the same scheme or an opposite hydrogen bond pattern.

clinic symmetry ($P2_1/c11$; McIver, 1963), the crystal structure is certainly triclinic ($P\bar{1}$). One of the most important reasons for this structural arrangement is related to the complex hydrogen bond scheme. McIver (1963) described it as presenting three «symmetric» bonds (O3···O3, O5···O6, and O4···O4), on the basis of the corresponding O···O distances. The results of the present refinement indicate that only two bonds may be considered «symmetric», *i.e*. the O3···O3 and O4···O4, although, as it was previously explained, the real arrangement of hydrogen bonds does not show any actually symmetric bond. As regards the atom pair O5, O6 we found a regular alternation between hydrogen bonds O5···O6 (2.58 Å) and non bonding contacts O6···O5 (3.26 Å). If the true symmetry of bultfonteinite had been monoclinic, these two distances should have been equal. In conclusion, the arrangement of hydrogen bonding is the main reason for the lowering of symmetry from monoclinic to triclinic. A neutron diffraction study is necessary to unravel the actual complexity of the hydrogen bond scheme of bultfonteinite.

Acknowledgments

The referee, Natale Perchiazzi, is thanked for his revision of the paper.

References

Bonazzi P., Bindi L., Medenbach O., Pagano R., Lampronti G.I., Menchetti S., 2007. Olmiite, $CaMn[SiO_3(OH)](OH)$, the Mn-dominant analogue of poldervaartite, a new mineral species from Kalahari manganese fields (Republic of South Africa). *Mineralogical Magazine* 71: 193-201.

Brese N.E., O'Keeffe M., 1991. Bond-valence parameters for solids. *Acta Crystallographica* B47: 192-197.

Buse B., Schumacher J.C., Sparks R.S.J., Field M., 2010. Growth of bultfonteinite and hydrogarnet in metasomatized basalt xenoliths in the B/K9 kimberlite, Damtshaa, Botswana: insights into hydrothermal metamorphism in kimberlite pipes. *Contributions to Mineralogy and Petrology* 160: 533-540.

Chakhmouradian A.R., Mitchell R.H., 2001. Three compositional varieties of perovskite from kimberlites of the Lac de Gras field (Northwest Territories, Canada). *Mineralogical Magazine* 65: 133-148.

Dai Y., Harlow G.E., McGhie A.R., 1993. Poldervaartite, $Ca(Ca_{0.5}Mn_{0.5})(SiO_3OH)(OH)$, a new acid nesosilicate from the Kalahari manganese field, South Africa: crystal structure and description. *American Mineralogist* 78: 1082-1087.

Ferraris G., Ivaldi G., 1988. Bond valence vs. bond length in O…O hydrogen bonds. *Acta Crystallographica* B44: 341-344.

Gross S., 1977. The mineralogy of the Hatrurim Formation, Israel. *Geological Survey of Israel Bulletin* 70, 130 pp.

Gutzmer J., Beukes N.J., 1996. Mineral paragenesis of the Kalahari manganese field, South Africa. *Ore Geology Reviews* 11: 405-428.

Kusachi I., Takechi Y., Henmi C., Kobayashi S., 1997. Borcarite from Fuka, Okayama Prefecture, Japan. *Mineralogical Journal* 19: 115-122.

Malik K.M.A., Jeffery J.W., 1976. A re-investigation of the structure of afwillite. *Acta Crystallographica* B32: 475-480.

McIver E.J., 1963. The structure of bultfonteinite, $Ca_4Si_2O_{10}F_2H_6$. *Acta Crystallographica* 16: 551-558.

Megaw, H.D., Kelsey, C.H., 1955. An accurate determination of the cell dimensions of bultfonteinite, $Ca_4Si_2O_{10}H_6F_2$. *Mineralogical Magazine* 30: 569-573.

Miyake H.J., 1965. In: Chukrov F.W., Bonshtedt-Kupletskaya M. (Eds.), 1972, *Mineraly* 3: 480.

Murdoch J., 1955. Bultfonteinite from Crestmore, California. *American Mineralogist* 46: 245-257.

Nyfeler D., Armbruster T., 1998. Silanol groups in minerals and inorganic compounds. *American Mineralogist* 83: 119-125.

Parry J., Williams A.F., Wright F.E., 1932. On bultfonteinite, a new fluorine-bearing hydrous calcium silicate from South Africa. *Mineralogical Magazine* 23: 145-162.

Sheldrick G.M., 2008. A short history of SHELX. *Acta Crystallographica* A64: 112-122.

Von Bezing K.L., Dixon R.D., Pohl D., Cavallo G., 1991. The Kalahari Manganese Field: an update. *Mineralogical Record* 22: 279-297.

(ms. pres. il 4 marzo 2011; ult. bozze il 10 maggio 2011)